CHEMISTRY
A EUROPEAN JOURNAL

DOI: 10.1002/chem.200902104

An Interpenetrated Framework Material with Hysteretic CO_2 Uptake

Karen L. Mulfort,[a, b] Omar K. Farha,[a] Christos D. Malliakas,[a] Mercouri G. Kanatzidis,[a] and Joseph T. Hupp*[a]

Abstract: A new, twofold interpenetrated metal–organic framework (MOF) material has been synthesized that demonstrates dramatic steps in the adsorption and hysteresis in the desorption of CO_2. Measurement of the structure by powder X-ray diffraction (PXRD) and pair distribution function (PDF) analysis indicates that structural changes upon CO_2 sorption most likely involve the interpenetrated frameworks moving with respect to each other.

Keywords: CO_2 adsorption · dynamic structures · gated sorption · hysteresis · metal–organic frameworks · porous materials

Introduction

The introduction and subsequent wide-reaching pursuit of new and exotic metal–organic frameworks (MOFs) has opened doors into the structural possibilities of crystalline, porous solid-state materials.[1,2] Scores of new MOF structures are now reported each year, and the ability to engender structural and chemical diversity with relative ease has long been recognized. However, once the metal nodes and organic ligands are arranged into the crystalline framework, their structure is largely stagnant. More recently, the ability of some of these *crystalline* materials to exhibit structural *flexibility* has been reported.[3] For example, several of the MIL materials from the Férey group exhibit a "breathing" mechanism upon solvent removal and subsequent pore filling with gas or vapor molecules.[4–7] In addition, technologically intriguing hysteretic H_2 uptake in flexible frameworks has been observed at both low[8] and high pressure.[9] The ability to effect guest-responsive structural behavior in traditionally crystalline MOF materials is becoming more apparent.[10–18] However, very few of these reports examine three-dimensional frameworks,[19] even fewer investigate catenated structures,[20] and most often, the reported flexible behavior is observed only at high pressure. A guest-responsive, structurally flexible porous material that demonstrates dynamic performance under more subtle conditions of pressure and temperature could have application potential in gas separations or as a highly selective sensor of molecular adsorbates.

Here we describe a new twofold catenated, pillared paddlewheel framework based on Zn^{II} coordination of a tetratopic carboxylate ligand and a linear dipyridyl ligand. The low-pressure CO_2 isotherms display a prominent step and a substantial repeatable hysteresis that together suggest dynamic structural behavior upon removal and re-adsorption of pore guests. Equally interestingly, high-pressure CO_2 isotherms indicate that these structural changes occur at technologically relevant conditions for CO_2 sequestration. We have verified the structural changes with the pair distribution function (PDF) method using high-energy synchrotron radiation. To our knowledge, the current study comprises the first application of this method to the problem of MOF structural dynamics. In contrast to CO_2, adsorption of both N_2 and Ar is characterized by a surprising gating effect, that is, virtually *no* adsorption at pressures less than the gate pressure. The differences suggest that two distinct types of dynamic structural change occur.

Results and Discussion

Synthesis and structure: We have previously described a library of pillared paddlewheel MOFs based upon mixed-ligand Zn^{II} coordination to linear dicarboxylates and dipyridyls.[21] In the present work, we have created a robust mate-

[a] K. L. Mulfort, Dr. O. K. Farha, Dr. C. D. Malliakas, Prof. M. G. Kanatzidis, Prof. J. T. Hupp
Department of Chemistry, Northwestern University
2145 Sheridan Road, Evanston, IL 60208 (USA)
Fax: (+1) 847-467-1425
E-mail: j-hupp@northwestern.edu

[b] K. L. Mulfort
Division of Chemical Sciences and Engineering
Argonne National Laboratory
9700 South Cass Avenue, Argonne, IL 60439 (USA)

Supporting information for this article is available on the WWW under http://dx.doi.org/10.1002/chem.200902104.

rial containing a tetratopic carboxylate ligand, 4,4′,4″,4‴-benzene-1,2,4,5-tetrayl-tetrabenzoic acid (**L1**).[22,23,24] We reasoned that this strut would yield a MOF structure containing relatively large pores and that the four-point connectivity would produce a structure exceptionally stable to guest removal. The linear dipyridyl ligand *N,N*′-di-(4-pyridyl)-1,4,5,8-naphthalenetetracarboxydiimide (**L2**) was used here since MOFs containing this ligand have likewise previously been shown to form robust structures.[25,26]

Static heating of **L1**, **L2**, and $Zn(NO_3)_2{\cdot}6H_2O$ in DMF at 80 °C for two days resulted in single crystals suitable for X-ray diffraction.[27] Analysis of the single-crystal data reveals a framework formula of Zn_2(**L1**)(**L2**) in two catenated networks, structure **1** in Figure 1B. As **1** is *y*ellow and incorporates the *o*cta-oxygen strut **L1**, we have denoted it as YO-MOF. **L1** bridges the Zn^{II} dimers and forms flat two-dimensional sheets. These perforated two-dimensional sheets are pillared by **L2**. However, unlike most other pillared paddlewheel structures we have encountered, these networks are interpenetrated as opposed to interwoven, such that the networks are maximally displaced from one another.[28] The **L2** pillars reside directly in the center of the diamond-shaped cavities formed by two of the **L1** ligands, and the substantial steric bulk of **L2** completely fills this space (Figure 2). This type of catenation results in a pore volume that is essentially halved from what would be observed in a single, non-catenated network.

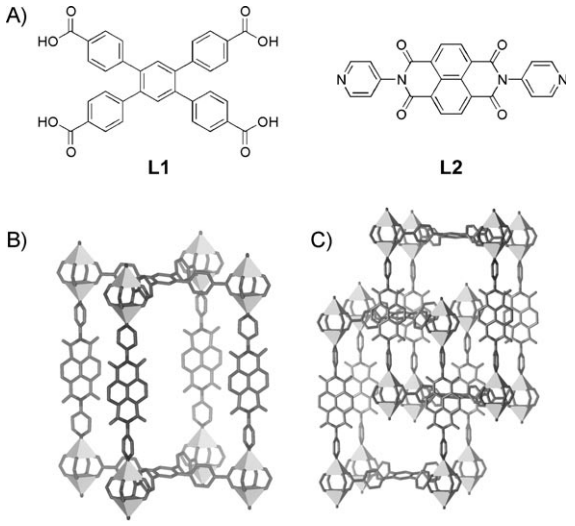

Figure 1. A) Chemical structure of **L1** and **L2**. B) Crystal structure of **1**, one level of catenation is omitted to illustrate connectivity. Polyhedra represent zinc ions; see Supporting Information for color figure. Hydrogens omitted for clarity. C) Catentation of **1**.

Despite the framework interpenetration, the structure retains 50% solvent accessible void volume as calculated by the SQUEEZE routine of PLATON.[29] Thermogravimetric analysis (TGA) of **1** reveals a 38% (by mass) loss of solvent, centered at 135 °C and complete by 200 °C (see the Supporting Information). Framework decomposition does not begin until 350 °C, indicating a comparatively high degree of stability for a large-pore paddlewheel-type MOF, most likely a direct result of the four-point binding of **L1**.

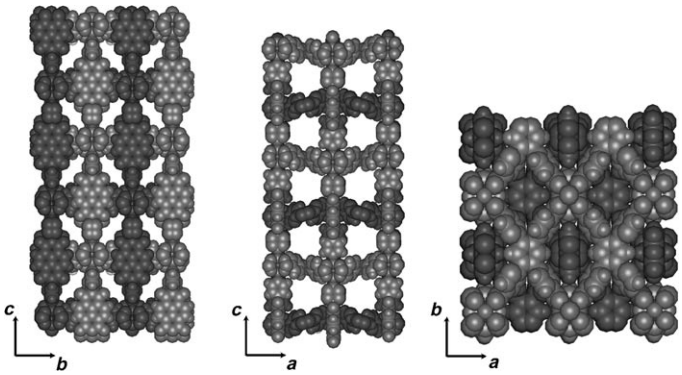

Figure 2. Packing diagrams of **1** (YO-MOF) in space-filling representation to illustrate interpenetration of two independent networks (dark and light).

CO_2, N_2, and Ar adsorption: Ultra-high capacity CO_2 uptake has been demonstrated in several MOF structures and is of immense technological interest for CO_2 storage and sequestration.[30–32] Additionally, a solid-state material that can selectively adsorb CO_2 from mixtures with other gases such as CH_4 or N_2 would have considerable potential in separations, perhaps most relevantly for flue gas decontamination. The low-pressure CO_2 isotherm of **1** at 273 K is presented in Figure 3A. The step in the isotherm at $P/P_o \approx 0.022$ is highly unusual, but not unprecedented.[4,16,33] The hysteresis is fully repeatable and is not simply a consequence of incomplete instrument equilibration (see the Supporting Information). The atypical CO_2 adsorption behavior at 273 K prompted us to measure isotherms at several temperatures (Figure 3B). The adsorption step and hysteresis move to higher absolute pressure with increasing temperature. Looking first at only the 273 K isotherm, it is difficult to judge if the jump in uptake is an effect of pore condensation or a true step in the isotherm. However, the isotherm measured at 263 K clearly displays an inflection in the step and appears to be approaching a plateau in the uptake. In the isotherms that display the step and hysteresis, the hysteresis loop is fully closed to rejoin the adsorption branch; all of the adsorbate molecules can be removed from the framework. Notably, above 278 K, the adsorption step and hysteresis are not observed before the pressure limit of these measurements. Plotting the adsorbed volume as a function of *relative* pressure (see the Supporting Information) rather than absolute pressure reveals that at elevated temperatures we simply have not reached the relative pressure necessary to observe the stepped adsorption behavior.

The hysteretic adsorption observed in YO-MOF could potentially provide a mechanism by which to adsorb CO_2 selectively from gas mixtures. To understand the framework's behavior under more technologically relevant conditions, we performed high-pressure measurements at various tempera-

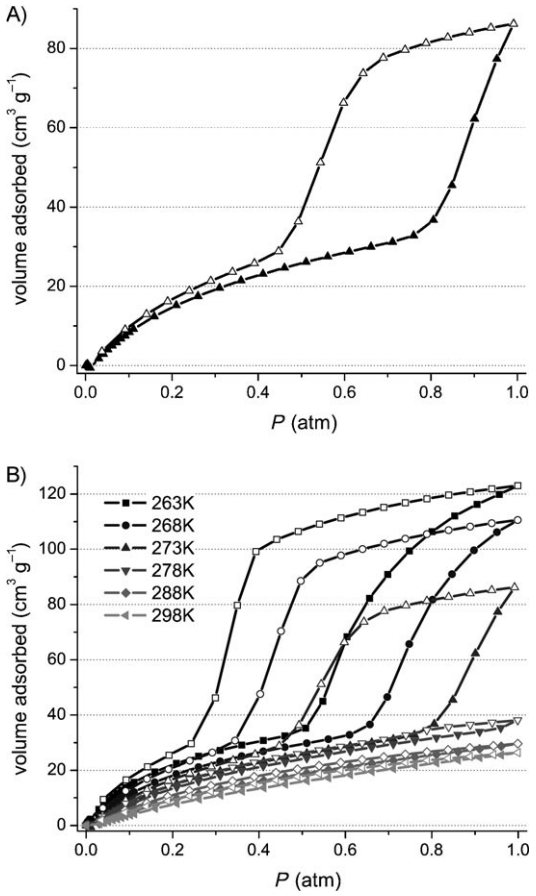

Figure 3. Low-pressure CO_2 isotherms of **1** (YO-MOF). A) 273 K, and B) temperatures from 263 K to 298 K. Closed symbols, adsorption; open symbols, desorption. Lines between data points are intended to guide the eye.

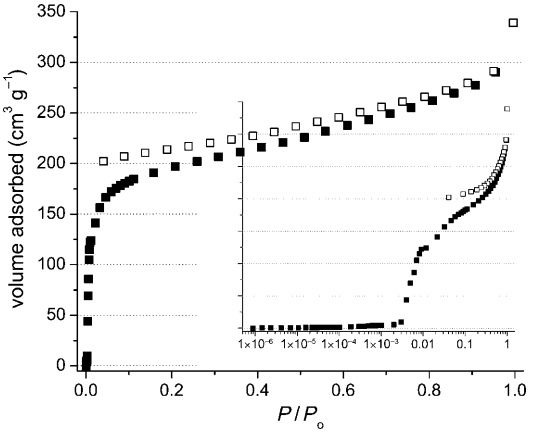

Figure 4. 77 K N_2 adsorption isotherm of **1** (YO-MOF). Closed symbols, adsorption; open symbols, desorption. Inset depicts adsorption/desorption on a log scale.

tures (see the Supporting Information). High-pressure CO_2 isotherms at elevated temperatures do indeed exhibit stepped adsorption, seen most clearly in 318 K and 328 K isotherms. As in the low-pressure studies, the position of the adsorption step is temperature dependent. This unusual stepped adsorption and hysteretic desorption, particularly at moderate pressures of 0.5 to 5 bar, has potential utility in separation processes. Notably, the capacity and hysteresis are retained over at least 15 adsorption/desorption cycles, further demonstrating the potential technological promise of YO-MOF and structures like it (see the Supporting Information).

Stepped CO_2 isotherms have been observed previously in high-pressure experiments, as well as modeled computationally, for selected IRMOF structures.[33] In these examples, the large step in the isotherm is attributed to attractive CO_2–CO_2 interactions within the framework. However, hysteresis on the desorption curve was not observed in the experiments or in the simulations. Broad and clearly resolved hysteresis loops are most often taken as indications of the presence of mesopores, as in the IUPAC Type IV isotherm classification.[34] The step in the adsorption branch of the isotherm in mesoporous materials results from capillary condensation within the pores near the saturation pressure. This behavior is well understood for N_2 and Ar adsorption at 77 K and 87 K up to 1 atm where the top of the isotherm represents adsorbate saturation. In contrast, the pressure at which we observe the step and hysteresis in the CO_2 isotherm is far below the saturation pressure (34.3 atm at 273 K), apparent in the high-pressure isotherms (see the Supporting Information). Similar behavior has been reported for the adsorption of nitrogen by a two-dimensional framework material[35] and by a three-dimensional pillared paddlewheel structure, but is otherwise unknown.[20,36]

The N_2 and Ar isotherms of YO-MOF display a fairly unusual gated adsorption behavior (see Figure 4 and the Supporting Information). Interestingly, there is virtually no adsorption until the gate pressure, at which point there is an abrupt increase in adsorption. Similar behavior has been reported in a two-dimensional layered coordination polymer,[37] but to our knowledge this behavior has not previously been observed in three-dimensional porous structures at low relative pressure.

The dynamic framework behavior responsible for the stepped CO_2 adsorption as well as gated N_2 and Ar adsorption could conceivably take any of several forms, including reversible: A) framework collapse, B) conversion between interpenetrated and interwoven catenate geometries, and/or C) strut (pillar) rotation; see Figure 5. The available static structural information (Figure 2) enables us to rule out Figure 5A as an important contributor: The YO-MOF networks are too tightly interpenetrated to allow significant framework collapse (i.e. orthorhombic distortion). Network/network packing constraints likewise strongly argue against Figure 5C, at least as sketched (however, see below). Further analysis requires dynamic structural information.

Pair distribution function (PDF) analysis: Lacking useable single-crystal data, powder X-ray diffraction (PXRD) was employed to monitor the dynamic behavior of **1** through the

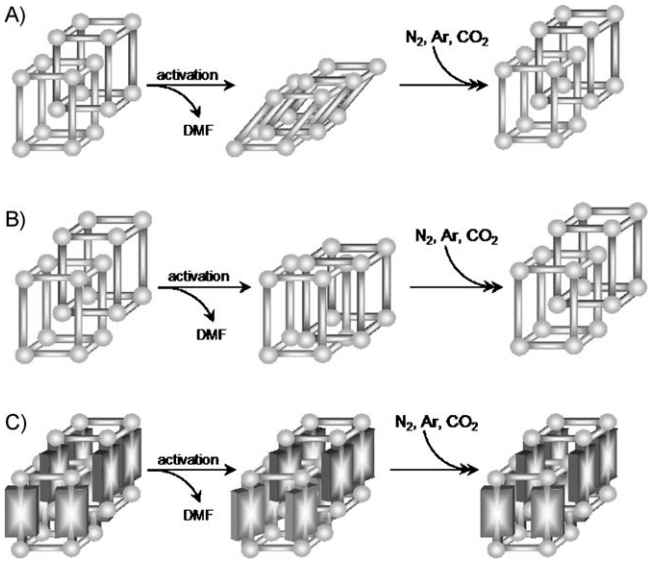

Figure 5. Candidate reversible structure changes of **1** (YO-MOF) upon activation and guest adsorption: A) framework collapse, B) shift between interpenetrated and interwoven geometries, C) pillar (strut) rotation.

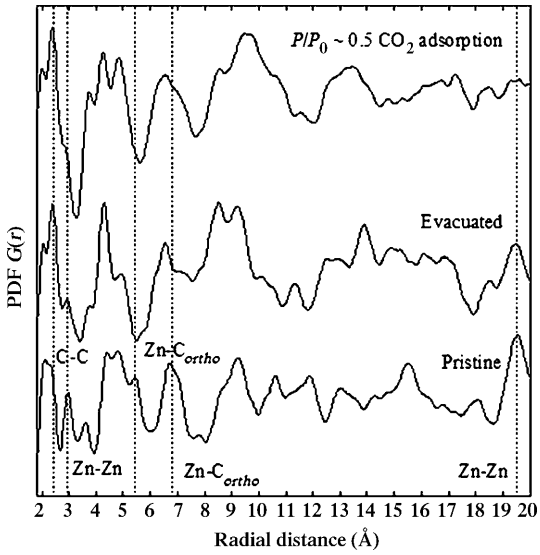

Figure 6. Pair distribution function analysis of pristine **1** (YO-MOF), evacuated (solvent free) and CO_2 treated material. Atomic pair correlations at around 2.5 Å belong to C–C, at about 3 Å to Zn–Zn, at about 5.5 Å and 6.7 Å to Zn–C_{ortho} (carbon atoms at the *ortho*-position of the benzene ring of **L1**), and at about 19.5 Å to Zn–Zn.

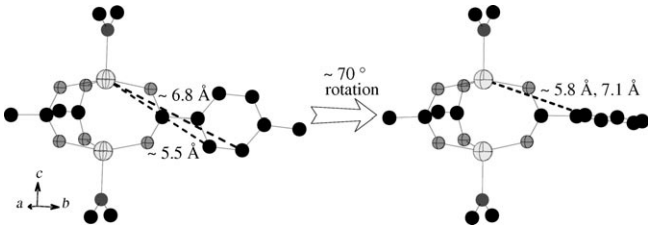

Figure 7. Proposed torsional motion of **L1** upon guest removal and re-adsorption.

hysteretic CO_2 adsorption/desorption cycle. The main difficulty with structural characterization of solvent-evacuated MOFs by single-crystal diffraction is the deterioration of the sharp Bragg reflections of the pristine material. To gain insight into the structure of the solvent-free (evacuated) and CO_2-treated compounds and also probe the origin of the hysteretic behavior we used the pair distribution function (PDF) technique.[38] Unlike other crystallographic techniques such as Rietveld, the PDF is a *total* scattering technique, which means that Bragg scattering and diffuse scattering are treated on an equal basis. Thus the PDF describes the distribution of inter-atomic distances in a material regardless of the degree of ordering. The technique is powerful in studying amorphous, poorly crystalline and disordered materials. To our knowledge this is the first example of the application of PDF analysis to problem of the local structure of MOFs.[39]

There are small but detectable differences (evident even in the powder diffraction pattern; see Figure S8 in the Supporting Information) between the initially prepared (solvent-filled) sample and the solvent-evacuated product. While differences are evident over a broad range of distances, those in the short-range region (<8 Å) are easier to distinguish and correlate to the framework structure than those in the long-range region. Assignment and interpretation of the latter are complicated by overlap of a multitude of interatomic interactions. Focusing on the short-range region, Figure 6 shows that the initially present atomic-pair correlations around 5.5 and 6.7 Å disappear in the evacuated compound. From simulated partial PDFs of the pristine structure (see the Supporting Information) these two vanished vectors belong, respectively, to distances between pairs of Zn atoms and between Zn and the *ortho*-C of the benzene rings of **L1**. Figure 7 illustrates the local motion responsible for the peak disappearances: rotation of a benzene ring of **L1** towards the plane that is normal to the pair of Zn atoms constituting a node.

The torsional motion in Figure 7 can be viewed as a variant of Figure 5C, involving the peripheral parts of **L1** rather than the diimide core. Perhaps more usefully, it can be viewed as an extra component of Figure 5B. Regardless, the PDF-detected distortion is induced by removal of the solvent and the structure remains in this conformation during the CO_2 adsorption/desorption.

At short range (<10 Å), the PDF of the CO_2 treated sample looks similar to that for the evacuated sample. At longer range, however, differences in the relative intensities of peaks and positions of correlations are apparent.[40] In particular, an initially strong peak at around 19.5 Å is diminished upon solvent removal and further diminished following CO_2 introduction (see Figure 6). Inspection of the single-crystal X-ray structure reveals a Zn–Zn separation matching this distance. While it is tempting to ascribe the observed peak evolution to changes in the Zn–Zn separation distance, this interpretation is unrealistic as the perti-

nent zinc ions are located in the same network, rather than adjacent networks; thus their separation distance is unaffected by framework/framework displacements or distortions. Simulations (see the Supporting Information) show, nevertheless, that conversion from interpenetrated to interwoven geometry (Figure 5B) is accompanied by a loss of intensity at 19.5 Å—consistent with experimental observations (Figure 6). The intensity loss, however, represents a composite of scattering effects involving many pairs of atoms, rather than a displacement of a single, easily identified pair.

With the PDF-supported structural descriptions in hand (Figure 5B and 7), we return to the unusual hysteretic adsorption behavior. We suggest that the CO_2 adsorption isotherms shown in Figure 3 can be viewed as an approximate sum of two Langmuir isotherms:[41] one that follows the adsorption branch and the other the desorption branch (see Figure S5 in the Supporting Informaiton). The surface area obtained from a simple Langmuir fit to the adsorption branch is $335\,m^2g^{-1}$ that obtained from the desorption branch is $690\,m^2g^{-1}$ NLDFT analysis[42] of the 273 K CO_2 isotherm from $0 < P < 0.75$ atm gives a surface area of $340\,m^2g,^{-1}$ in excellent agreement with the Langmuir fit. (The Langmuir approach is used solely for convenience and is not meant to imply microscopic validity of the underlying "monolayer adsorption" model.) The surface area value returned from the adsorption branch indicates that there is substantial CO_2-accessible internal surface area. Upon complete removal of guest solvent molecules, it is not unrealistic for the frameworks to shift towards each other to become inter*woven* (recall that the solvent-containing crystal structure is fully inter*penetrated*) and maximize favorable framework-framework van der Waals interactions.

Conclusions

While not without precedent, the adsorption behavior of **1** described here is rare in crystalline materials and not yet well understood. The CO_2 isotherms display stepped adsorption and hysteresis, which have been observed previously at high pressures in MOF materials (generally above 5–10 bar). But, this adsorption behavior begins much earlier in **1**, near $P/P_o \sim 0.02$, or approximately 0.5–2 bar for all temperatures studied.

Additionally, the gating behavior observed in the N_2 and Ar isotherms has not previously been reported at low pressures for a three-dimensional MOF structure. Taken together, the adsorption results, supported by PDF data, qualitatively point to dynamic framework behavior upon both solvent removal (activation) and introduction of adsorbate molecules. The nature of the dynamic behavior appears to be dominated by inter-conversion between interpenetrated and interwoven geometries, with accompanying sizable changes in guest-accessible surface area, as exemplified in Figure 5B and refined in Figure 7.

In notable contrast to most other examples of dynamic framework behavior, the interconversions here are robust, with the material retaining essentially all its porosity even after more than a dozen cycles. The robustness is no doubt a consequence of the *absence* of torque or other strain on individual chemical bonds; instead the relevant displacements occur at the supramolecular and network level, or else involve low-energy torsional motions. As technological requirements demand more specificity in materials properties, solid framework materials with the ability to display flexibility upon guest removal and adsorption will no doubt enjoy immense attention as solutions to extant challenges in chemical separations and other areas.

Experimental Section

General methods and materials: All commercial reagents were of ACS grade and purchased from Sigma–Aldrich unless otherwise noted. Powder X-ray diffraction (PXRD) patterns were recorded with a Rigaku XDS 2000 diffractometer using nickel-filtered $Cu_{K\alpha}$ radiation ($\lambda =$ 1.5418 Å) over a range of $5° < 2\theta < 40°$ in 0.1° steps with a 1 s counting time per step. Powder samples were placed in the diffractometer mounted on a ground glass sample holder. Thermogravimetric analyses (TGA) were performed on a Mettler-Toledo TGA/SDTA851e. Samples (3–5 mg) in alumina pans were heated from 25 °C to 700 °C at 10 °C/minute under N_2. Elemental analyses were performed by Atlantic Microlabs, Inc. (Norcross, GA). The syntheses of **L1**[43] and **L2**[44] have been previously reported.

Synthesis and characterization of 1 (YO-MOF): Single crystals of **1** were obtained by the static heating of $Zn(NO_3)_2{\cdot}6H_2O$ (42 mg, 0.14 mmol), **L1** (75 mg, 0.14 mmol), and **L2** (30 mg, 0.07 mmol) in DMF (15 mL), and divided between four 2 dram vials. The vials were placed in an 80 °C oven for two days, over which time yellow block crystals of **1** formed.

A single crystal of **1** was mounted on a BRUKER APEX2 V2.1–0 diffractometer equipped with a graphite-monochromated $Mo_{K\alpha}$ ($\lambda = 0.71073$ Å) radiation source in a cold nitrogen stream. All crystallographic data were corrected for Lorentz and polarization effects (SAINT). The structures were solved by direct methods and refined by the full-matrix least-squares method on $F2$ with appropriate software implemented in the SHELXTL program package. Most of the guest DMF solvent molecules within the pores are severely disordered, which hindered satisfactory development of the model; therefore, the SQUEEZE routine in PLATON was applied to remove the contributions of electron density from disordered solvent molecules. The outputs from the SQUEEZE calculations are attached to the CIF file. One of the pyridyl groups of **L2** was disordered over two positions, this is reflected in the CIF file. All of the non-hydrogen atoms were refined anisotropically. CCDC-704474 contains the supplementary crystallographic data for this paper. These data can be obtained free of charge from The Cambridge Crystallographic Data Centre via www.ccdc.cam.ac.uk/data_request/cif

A large scale preparation of **1** was developed for adsorption studies. A sample preparation of **1** follows: $Zn(NO_3)_2{\cdot}6H_2O$ (167 mg, 0.56 mmol), **L1** (300 mg, 0.54 mmol), and **L2** (120 mg, 0.28 mmol) were dissolved in DMF (60 mL). This solution was divided equally between sixteen two-dram screw cap vials and heated to 80 °C for two days. The warm mother liquor was decanted, the yellow microcrystalline powder was washed with fresh DMF and the solid material was stored under fresh DMF until characterization by PXRD and TGA. Yield **1**: 80 mg, 26% based on Zn. Elemental analysis calcd (%) for **1·4H$_2$O**, $C_{58}H_{38}N_4O_{16}Zn_2$: C 59.15, H 3.25, N 4.76; found: C 58.80, H 3.25, N 4.76.

Low-pressure adsorption measurements: Low-pressure carbon dioxide, nitrogen, and argon adsorption measurements were performed using an Autosorb 1-MP from Quantachrome Instruments. Ultra-high purity grade He, N_2, and Ar and research grade CO_2 were used for all adsorption measurements. Prior to analysis, materials were soaked in THF to exchange the synthesis solvent (DMF). The THF solution was refreshed

several times over one day. Samples of **1** were the loaded into a sample tube of known weight and activated at room temperature and dynamic vacuum for about 24 h to completely remove guest solvents. After activation, the sample and tube were re-weighed to obtain the precise mass of the evacuated sample. CO_2 adsorption isotherms were measured at temperatures between 263 K and 298 K, the temperature was held constant using an isothermal water bath. N_2 adsorption isotherms were measured at 77 K (liquid N_2 bath) and Ar adsorption isotherms were measured at 87 K (liquid Ar bath).

Acknowledgements

We thank Dr. Matthias Thommes of Quantachrome, Inc. for valuable discussions. We acknowledge Argonne National Laboratory (Lab-Grad fellowship for K.L.M.), the U.S. Dept. of Energy's Office of Science (grant no. DE-FG02-08ER15967), and the Northwestern Nanoscale Science and Engineering Center for financial support of this research. Use of the Advanced Photon Source (APS) was supported by the U.S. Department of Energy, Office of Science, Office of Basic Energy Sciences, under Contract No. DE-AC02–06CH11357. The PDF work was conducted at the Midwest Universities Collaborative Access Team (MUCAT) sector 6-ID-D at the APS that is supported by the U.S. Department of Energy, Office of Science, Office of Basic Energy Sciences, through the Ames Laboratory under Contract No. W-7405-Eng-82.

[1] G. Férey, *Chem. Soc. Rev.* **2008**, *37*, 191–214.
[2] S. Kitagawa, R. Kitaura, S. Noro, *Angew. Chem.* **2004**, *116*, 2388–2430; *Angew. Chem. Int. Ed.* **2004**, *43*, 2334–2375.
[3] S. Kitagawa, K. Uemura, *Chem. Soc. Rev.* **2005**, *34*, 109–119.
[4] S. Bourrelly, P. L. Llewellyn, C. Serre, F. Millange, T. Loiseau, G. Férey, *J. Am. Chem. Soc.* **2005**, *127*, 13519–13521.
[5] P. L. Llewellyn, S. Bourrelly, C. Serre, Y. Filinchuk, G. Férey, *Angew. Chem.* **2006**, *118*, 7915–7918; *Angew. Chem. Int. Ed.* **2006**, *45*, 7751–7754.
[6] C. Serre, S. Bourrelly, A. Vimont, N. A. Ramsahye, G. Maurin, P. L. Llewellyn, M. Daturi, Y. Filinchuk, O. Leynaud, P. Barnes, G. Férey, *Adv. Mater.* **2007**, *19*, 2246–2251.
[7] C. Serre, C. Mellot-Draznieks, S. Surble, N. Audebrand, Y. Filinchuk, G. Férey, *Science* **2007**, *315*, 1828–1831.
[8] X. B. Zhao, B. Xiao, A. J. Fletcher, K. M. Thomas, D. Bradshaw, M. J. Rosseinsky, *Science* **2004**, *306*, 1012–1015.
[9] H. J. Choi, M. Dinca, J. R. Long, *J. Am. Chem. Soc.* **2008**, *130*, 7848–7850.
[10] E. Cussen, J. B. Claridge, M. J. Rosseinsky, C. J. Kepert, *J. Am. Chem. Soc.* **2002**, *124*, 9574–9581.
[11] A. J. Fletcher, E. J. Cussen, T. J. Prior, M. J. Rosseinsky, C. J. Kepert, K. M. Thomas, *J. Am. Chem. Soc.* **2001**, *123*, 10001–10011.
[12] S. Onishi, T. Ohmori, T. Ohkubo, H. Noguchi, L. Di, Y. Hanzawa, H. Kanoh, K. Kaneko, *Appl. Surf. Sci.* **2002**, *196*, 81–88.
[13] D. Tanaka, K. Nakagawa, M. Higuchi, S. Horike, Y. Kubota, T. C. Kobayashi, M. Takata, S. Kitagawa, *Angew. Chem.* **2008**, *120*, 3978–3982; *Angew. Chem. Int. Ed.* **2008**, *47*, 3914–3918.
[14] K. Uemura, R. Matsuda, S. Kitagawa, *J. Solid State Chem.* **2005**, *178*, 2420–2429.
[15] S. Ma, D. Sun, X.-S. Wang, H.-C. Zhou, *Angew. Chem.* **2007**, *119*, 2510–2514; *Angew. Chem. Int. Ed.* **2007**, *46*, 2458–2462.
[16] P. K. Thallapally, J. Tian, M. Radha Kishan, C. A. Fernandez, S. J. Dalgarno, P. B. McGrail, J. E. Warren, J. L. Atwood, *J. Am. Chem. Soc.* **2008**, *130*, 16842–16843.
[17] C. J. Kepert, M. J. Rosseinsky, *Chem. Commun.* **1999**, 375–376.
[18] B. Chen, C. Liang, J. Yang, D. S. Contreras, Y. L. Clancy, E. B. Lobkovsky, O. M. Yaghi, S. Dai, *Angew. Chem.* **2006**, *118*, 1418–1421; *Angew. Chem. Int. Ed.* **2006**, *45*, 1390–1393.
[19] J. T. Culp, M. R. Smith, E. Bittner, B. Bockrath, *J. Am. Chem. Soc.* **2008**, *130*, 12427–12434.
[20] R. Kitaura, G. Akiyama, K. Seki, S. Kitagawa, *Angew. Chem.* **2003**, *115*, 444–447; *Angew. Chem. Int. Ed.* **2003**, *42*, 428–431.
[21] B. Q. Ma, K. L. Mulfort, J. T. Hupp, *Inorg. Chem.* **2005**, *44*, 4912–4914.
[22] O. K. Farha, K. L. Mulfort, J. T. Hupp, *Inorg. Chem.* **2008**, *47*, 10223–10225.
[23] A. M. Shultz, O. K. Farha, J. T. Hupp, S. T. Nguyen, *J. Am. Chem. Soc.* **2009**, *131*, 4204–4205.
[24] For examples of related tetratopic struts, see: X. Lin, J. Jia, X. Zhao, K. M. Thomas, A. J. Blake, G. S. Walker, N. R. Champness, P. Hubberstey, M. Schröder, *Angew. Chem.* **2006**, *118*, 7518–7524; *Angew. Chem. Int. Ed.* **2006**, *45*, 7358–7364 and L. Ma, W. Lin, *J. Am. Chem. Soc.* **2008**, *130*, 13834–13835.
[25] K. L. Mulfort, J. T. Hupp, *J. Am. Chem. Soc.* **2007**, *129*, 9604–9605.
[26] K. L. Mulfort, J. T. Hupp, *Inorg. Chem.* **2008**, *47*, 7936–7938.
[27] Single crystal data for **1**: $C_{29}H_{13}N_2O_6Zn$, $M=550.78$, orthorhombic, *Imma*, $a=22.898(13)$, $b=15.668(9)$, $c=22.389(12)$ Å, $V=8032(8)$ Å^3, $Z=8$, $\rho_{cald}=0.911$, $\mu=0.00016(4)$, $F(000)=2232$, GOF = 1.107. $R1$ and w$R2$ are 0.0659 and 0.0792, respectively for 216 parameters and 3917 reflections [$I>2\sigma(I)$].
[28] J. L. C. Rowsell, O. M. Yaghi, *Microporous Mesoporous Mater.* **2004**, *73*, 3–14.
[29] A. L. Spek, *J. Appl. Crystallogr.* **2003**, *36*, 7–13.
[30] P. L. Llewellyn, S. Bourrelly, C. Serre, A. Vimont, M. Daturi, L. Hamon, G. De Weireld, J.-S. Chang, D.-Y. Hong, Y. Kyu Hwang, S. Hwa Jhung, G. Férey, *Langmuir* **2008**, *24*, 7245–7250.
[31] S. R. Caskey, A. G. Wong-Foy, A. J. Matzger, *J. Am. Chem. Soc.* **2008**, *130*, 10870–10871.
[32] A. R. Millward, O. M. Yaghi, *J. Am. Chem. Soc.* **2005**, *127*, 17998–17999.
[33] K. S. Walton, A. R. Millward, D. Dubbeldam, H. Frost, J. J. Low, O. M. Yaghi, R. Q. Snurr, *J. Am. Chem. Soc.* **2008**, *130*, 406–407.
[34] K. S. W. Sing, D. H. Everett, R. A. W. Haul, L. Moscou, R. A. Pierotti, J. Rouquerol, T. Siemieniewska, *Pure Appl. Chem.* **1985**, *57*, 603–619.
[35] A. Kondo, H. Noguchi, L. Carlucci, D. M. Proserpio, G. Ciani, H. Kajiro, T. Ohba, H. Kanoh, K. Kaneko, *J. Am. Chem. Soc.* **2007**, *129*, 12362–12363.
[36] K. Seki, *Phys. Chem. Chem. Phys.* **2002**, *4*, 1968–1971.
[37] D. Li, K. Kaneko, *Chem. Phys. Lett.* **2001**, *335*, 50–56.
[38] S. J. L. Billinge, M. G. Kanatzidis, *Chem. Commun.* **2004**, 749–760.
[39] While not involving a MOF material, the successful application of differential PDF methods to the problem of N_2 adsorption of a porous Prussian blue material should be noted; see K. W. Chapman, P. J. Chupas, C. J. Kepert, *J. Am. Chem. Soc.* **2005**, *127*, 11232–11233.
[40] More details about the structural characterization by PDF can be found in the Supporting Information.
[41] I. Langmuir, *J. Am. Chem. Soc.* **1918**, *40*, 1361–1403.
[42] J. Jagiello, M. Thommes, *Carbon* **2004**, *42*, 1227–1232.
[43] P. H. Dinolfo, M. E. Williams, C. L. Stern, J. T. Hupp, *J. Am. Chem. Soc.* **2004**, *126*, 12989–13001.
[44] O. K. Farha, K. L. Mulfort, J. T. Hupp, *Inorg. Chem.* **2008**, *47*, 10223–10225.

Received: July 28, 2009
Published online: November 13, 2009

